 ©2011 Kvantovaya Elektronika and Turpion Ltd

CONTROL OF LASER RADIATION PARAMETERS

PACS numbers: 42.55.Px; 42.62.Eh; 06.20.–f
DOI: 10.1070/QE2011v041n08ABEH014588

Spectral characteristics of a laser emitter designed for pumping and detecting a reference quantum transition of a caesium frequency standard

A.V. Ivanov, V.D. Kurnosov, K.V. Kurnosov, V.I. Romantsevich, R.V. Chernov, A.A. Marmalyuk, N.A. Volkov, V.S. Zholnerov

***Abstract*. Experimental and calculated spectral characteristics of a diode laser with a Bragg grating soldered on a thermoelectric cooler are presented. A model of the laser is developed, which takes into account the pressure arising after soldering the Bragg grating on the thermoelectric cooler, as well as temperature and dispersion. Theoretical and experimental spectral characteristics of the laser are compared and their satisfactory agreement is shown.**

Keywords: *frequency standard, single-frequency laser, Bragg diffraction grating, D_2 line of the caesium atom.*

1. Introduction

Development of laser emitters used as highly stable sources of resonance radiation for pumping and detecting the reference quantum transition in quantum frequency standards based on beams and vapours of caesium (^{133}Cs) and rubidium (^{87}Rb) atoms is an important direction providing further improvement of technical characteristics of global navigation satellite systems GPS and GLONASS.

For optical pumping and detection of a quantum transition the authors of paper [1] proposed a special design of a single-frequency laser with a fibre Bragg grating (FBG). The laser diode (LD) and FBG are mounted on two separate thermoelectric coolers (TECs), which allow for independent tuning to the D_2 line of the caesium atom. Zhuravleva et al. [2] proposed a model for calculating spectral characteristics of the LD with a FBG and demonstrated that the laser wavelength can be varied by changing the pump current and temperature of the LD and the FBG. In these studies, use was made of the technology for attaching the FBG to the TEC using elastosil. However, in the case of lasers designed to operate in space, it is desirable to solder metallised fibres with FBGs to TECs instead of using elastosil.

In this paper, we study both theoretically and experimentally the spectral characteristics of the laser emitter in which the fibre is soldered to the TEC using the POIN-52 solder (tin, 48 %; indium, 52 %).

One of the key elements of atomic-beam tubes (ABTs) for quantum frequency standards is an automatic frequency control (AFC) system, operating under different external influences, namely climatic and mechanical effects. Therefore, the developers of ABTs are primarily interested in the dependence of the laser wavelength on its pump current and temperature and on the FBG temperature.

During the laser operation its pump current increases due to a gradual degradation of the LD, and at some current there occurs a moment when the laser wavelength switches to the adjacent mode and no longer coincides with the absorption line of the caesium atom. To avoid this, it is necessary to change the temperature of either LD or FBG. So the question arises: which of these parameters should be controlled in constructing the AFC? To answer this question, in this work we study both experimentally and theoretically the dependence of the LD wavelength on the temperature of the LD and FBG. Our calculations will be based on the model described in [2].

2. Model of a laser diode with a fibre Bragg grating

The scheme of an FBG laser diode is presented in Fig. 1. The field in the cavity can be written in the form [2]:

$$U_i(z) = \begin{cases} A_i \sin[\beta_{1i}(z+L)], & -L \leqslant z \leqslant -(L_2+L_3), \\ B_i \sin(\beta_{3i}z) + C_i \cos(\beta_{3i}z), & -(L_2+L_3) \leqslant z \leqslant -L_2, \\ D_i \sin(\beta_{2i}z) + E_i \cos(\beta_{2i}z), & -L_2 \leqslant z \leqslant 0, \\ [R_i(z) - S_i(z)] \sin[\beta_0(z-L_B)], & 0 \leqslant z \leqslant L_B, \end{cases} \quad (1)$$

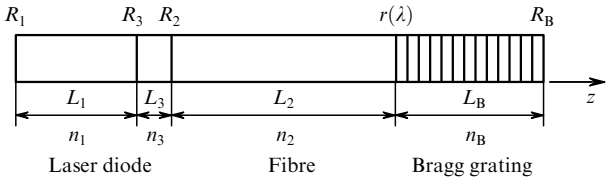

Figure 1. Scheme of a laser diode with a Bragg grating in the fibre (L_1, n_1, L_2, n_2, L_3, n_3, L_B, n_B are the lengths and refractive indices of the laser diode, optical fibre, air gap, and FBG; R_1, R_2, R_3, R_B are the reflectances; $r(\lambda)$ is the reflectance at the optical fibre – Bragg grating interface).

A.V. Ivanov, V.D. Kurnosov, K.V. Kurnosov, V.I. Romantsevich, R.V. Chernov, A.A. Marmalyuk, N.A. Volkov Federal State Unitary Enterprise 'M.F. Stelmakh Polyus Research and Development Institute', ul. Vvedenskogo 3, 117342 Moscow, Russia; e-mail: webeks@mail.ru, marm@siplus.ru;
V.S. Zholnerov JSC 'RIRT', pl. Rastrelli 2, 191124 St. Petersburg, Russia

Received 18 March 2011; revision received 7 June 2011
Kvantovaya Elektronika **41** (8) 692 – 696 (2011)
Translated by I.A. Ulitkin

where $\beta_{1i} = 2\pi n_1/\lambda_i$, $\beta_{2i} = 2\pi n_2/\lambda_i$, $\beta_{3i} = 2\pi n_3/\lambda_i$, $\beta_0 = 2\pi n_B/\lambda_B$ are the propagation constants in the corresponding regions; λ_B is the Bragg wavelength; and $L = L_1 + L_2 + L_3$. In (1) the boundary conditions $U_i(-L) = U_i(L_B) = 0$. The coefficients A_i, B_i, C_i D_i, E_i are independent of z.

The expressions for the coefficients $R_i(z)$ and $S_i(z)$ are borrowed from papers [3, 4]:

$$R_i(z) = R(0)\,\frac{\gamma_i \cosh[\gamma_i(z - L_B)] - \theta_i \sinh[\gamma_i(z - L_B)]}{\gamma_i \cosh(\gamma_i L_B) + \theta_i \sinh(\gamma_i L_B)}, \quad (2)$$

$$S_i(z) = R(0)\,\frac{\gamma_{1i} \cosh[\gamma_i(z - L_B)] + \chi_i \sinh[\gamma_i(z - L_B)]}{\gamma_i \cosh(\gamma_i L_B) + \theta_i \sinh(\gamma_i L_B)}. \quad (3)$$

The reflectance at the fibre – FBG interface ($z = 0$) is calculated from the expression

$$r = \frac{S(0)}{R(0)} = \frac{\gamma_{1i} \cosh(\gamma_i L_B) - \chi_i \sinh(\gamma_i L_B)}{\gamma_i \cosh(\gamma_i L_B) + \theta_i \sinh(\gamma_i L_B)}, \quad (4)$$

the power reflectance being $R = |r|^2$.

The coefficients entering (2)–(4) are defined by the expressions

$$\gamma_i^2 = \left(\frac{\alpha_B}{2} + j\delta_i\right)^2 + K_0^2, \quad \delta_i = \beta_i - \beta_0 = 2\pi n_B\left(\frac{1}{\lambda_i} - \frac{1}{\lambda_B}\right),$$

$$\gamma_{1i} = \xi\gamma_i, \quad \xi = r_0 \exp(-j2\beta_0 L_B), \quad r_0 = \sqrt{R_B}, \quad (5)$$

$$\theta_i = \left(\frac{\alpha_B}{2} + j\delta_i\right) + jK_0\xi, \quad \chi_i = \left(\frac{\alpha_B}{2} + j\delta_i\right)\xi + jK_0,$$

where γ_i is the dispersion relation; α_B is the FBG loss; K_0 is coupling coefficient between counterpropagating waves.

By sewing together the solutions for the field $U_i(z)$ and the derivative $dU_i(z)/dz$ at points $z = 0$, $-L_2$, $-(L_2 + L_3)$, we obtain the characteristic equation determining the radiation wavelengths that can propagate in the system shown in Fig. 1:

$$a_{1i}d_{2i} + a_{2i}d_{1i} - f_i(b_{1i}d_{2i} + d_{1i}b_{2i}) = 0. \quad (6)$$

The coefficients a_{1i}, a_{2i}, b_{1i}, b_{2i}, d_{1i}, d_{2i}, f_i are found from expressions (7) and (8) from paper [2].

The averaged photon density in the cavity of the laser emitter [2] is

$$S_i = \frac{V_1}{V_\Sigma}\,\beta R_{sp}\left\{c_0\left[\frac{1}{n_1}F_{1i}(\alpha_{1\Sigma} - \Gamma_a g_i) + \frac{1}{n_2}F_{2i}\alpha_{2\Sigma} + \frac{1}{n_3}F_{3i}\alpha_{3\Sigma} + \frac{1}{n_B}F_B\alpha_{B\Sigma}\right]\right\}^{-1}, \quad (7)$$

and the photon density in the LD cavity is

$$S_{1i} = \frac{V_\Sigma}{V_1}F_{1i}S_i, \quad (8)$$

where c_0 is the speed of light in vacuum; Γ_a is the optical confinement factor; β is the coefficient taking into account spontaneous emission in the generated mode; V_i is the volume of the active medium of the LD; V_Σ is the total volume of the laser emitter.

The coefficients F_{ij}, optical losses α_i, gain g_i and spontaneous recombination rate R_{sp} are found from expressions (18), (20), (22) and (24) from paper [2].

Optical power at the LD cavity output with the reflectance R_1 is

$$P = h\nu\,\frac{c_0}{n_{1gr}}\,A_c(1 - R_1)\sum_i S_{1i}, \quad (9)$$

where A_c is the cross-sectional area of the emitting laser region; n_{1gr} is the group refractive index in the LD.

3. Accounting for the effects of pressure, temperature, and dispersion on the Bragg wavelength of radiation

In studying the effect of the pressure on the shift of the Bragg wavelength we will use the results of paper [5]. The Bragg wavelength is

$$\lambda_B(T_0) = 2n_{B0}\Lambda(T_0), \quad (10)$$

where $n_{B0} = n_B(T_0)$ is the effective FBG index at temperature T_0; $\Lambda(T_0)$ is the period of the refractive index modulation of the fibre grating; T_0 is the ambient temperature.

Change in the λ_B with pressure is found from

$$\Delta\lambda_{Bp}(T_0) = \lambda_B(T_0)\left[\frac{1}{\Lambda(T_0)}\frac{\partial\Lambda}{\partial P} + \frac{1}{n_{B0}}\frac{\partial n_B}{\partial P}\right]\Delta P, \quad (11)$$

where

$$\frac{1}{\Lambda(T_0)}\frac{\partial\Lambda}{\partial P} = -\frac{1 - 2\mu}{E}; \quad \frac{1}{n_{B0}}\frac{\partial n_B}{\partial P} = \frac{n_{B0}^2}{2E}(1 - 2\mu)(2\rho_{12} + \rho_{11}); \quad (12)$$

μ is Poisson's ratio; E is Young's modulus; ρ_{11}, ρ_{12} are Pockels coefficients of the elastooptic tensor; ΔP is the pressure increment after soldering the FBG to the TEC. Using formulas (11), (12) we can determine the pressure increment ΔP, which is obtained after cooling the FBG to the temperature T_0.

With changing the FBG temperature, $\Delta\lambda_{Bp}$ changes. When the FBG temperature is equal to the fusion temperature T_{fus} of the solder, which is used for soldering the FBG to the TEC, the quantity $\Delta\lambda_{Bp}$ will be equal to zero. Suppose that $\Delta\lambda_{Bp}$ is linearly dependent on the FBG temperature, then

$$\Delta\lambda_{Bp}(T_B) = \lambda_B(T_0)K_p, \quad (13)$$

where

$$K_p = \left(\frac{1}{\Lambda(T_0)}\frac{\partial\Lambda}{\partial P} + \frac{1}{n_{B0}}\frac{\partial n_B}{\partial P}\right)\Delta P\left(1 - \frac{T_B - T_0}{T_{fus} - T_0}\right);$$

T_B is the FBG temperature. At $T_B = T_0$, expression (13) transforms into (11).

The temperature change in the period of the refractive index modulation has the form

$$\Lambda(T_B) = \Lambda(T_0)\left[1 + \alpha_{Bt}(T_B - T_0) + \frac{1}{\Lambda(T_0)}\frac{\partial\Lambda}{\partial P} \times\right.$$

$$\times \Delta P\left(1-\frac{T_{\rm B}-T_0}{T_{\rm fus}-T_0}\right)\Bigg], \quad (14)$$

where $\alpha_{\rm Bt}$ is the linear expansion coefficient of the FBG.

The dependence of the FBG index on the temperature, pressure and dispersion is defined as

$$n_{\rm B}(T_{\rm B}) = n_{\rm B}(T_0)\Bigg\{1+\frac{1}{n_{\rm B0}}\frac{\partial n_{\rm B}}{\partial T_{\rm B}}(T_{\rm B}-T_0)+\frac{1}{n_{\rm B0}}\frac{\partial n_{\rm B}}{\partial P}$$

$$\times \Delta P\left(1-\frac{T_{\rm B}-T_0}{T_{\rm fus}-T_0}\right)+\frac{1}{n_{\rm B0}}\frac{\partial n_{\rm B}}{\partial \lambda}[\lambda-\lambda_{\rm B}(T_0)]\Bigg\}. \quad (15)$$

For $\lambda = \lambda_{\rm B}(T_{\rm B})$ with account for $\lambda_{\rm B}(T_{\rm B}) = 2n_{\rm B}(T_{\rm B})\Lambda(T_{\rm B})$ we have

$$\lambda_{\rm B}(T_{\rm B}) = \lambda_{\rm B}(T_0)(1+K)^{-1}(1+K_{\rm t}+K_{\rm p}+K), \quad (16)$$

where

$$K_{\rm t} = \left(\alpha_{\rm Bt}+\frac{1}{n_{\rm B0}}\frac{\partial n_{\rm B}}{\partial T_{\rm B}}\right)(T_{\rm B}-T_0); \quad K = -\frac{1}{n_{\rm B0}}\frac{\partial n_{\rm B}}{\partial \lambda}\lambda_{\rm B}(T_0).$$

When considering the dependence of the spectral characteristics of the laser on the temperature changes of the LD, the refractive index of the LD at a constant FBG temperature can be written as

$$n_1(T_{\rm LD}) = n_{10}\Bigg\{1+\frac{1}{n_{10}}\frac{\partial n_1}{\partial \lambda}[\lambda-\lambda_{\rm B}(T_0)]$$

$$+\frac{1}{n_{10}}\left(\frac{\partial n_1}{\partial T_{\rm LD}}+\Gamma_{\rm a}\frac{\partial n_1}{\partial n_{\rm a}}\frac{\partial n_{\rm a}}{\partial T_{\rm LD}}\right)(T_{\rm LD}-T_0)\Bigg\}, \quad (17)$$

where n_{10} is the refractive index of the LD at $T_{\rm LD} = T_0$ and $\lambda = \lambda_{\rm B}(T_0)$; $T_{\rm LD}$ is the LD temperature; $\partial n_1/\partial n_{\rm a}$ is a change in the refractive index of the LD with changing the carrier density in the active region of the laser; $\partial n_{\rm a}/\partial T_{\rm LD}$ is a change in the carrier density with changing the LD temperature.

In this paper we consider the ambient temperature T_0 to be fixed (only the temperature of the LD or FBG changes) and, therefore, the fibre index n_2 (see Fig. 1) depends only on the dispersion:

$$n_2(\lambda) = n_{20}\Bigg\{1+\frac{1}{n_{20}}\frac{\partial n_2}{\partial \lambda}[\lambda-\lambda_{\rm B}(T_0)]\Bigg\}, \quad (18)$$

where n_{20} is the fibre index at $T = T_0$ and $\lambda = \lambda_{\rm B}(T_0)$. The refractive index of the air gap is $n_3 = 1$.

We assume that $\Delta L_{\rm B}/L_{\rm B} = \Delta\Lambda/\Lambda$ [5] and, therefore, the temperature dependence of the Bragg grating length can be written in the form

$$L_{\rm B}(T_{\rm B}) = L_{\rm B}(T_0)\Bigg[1+\alpha_{\rm Bt}(T_{\rm B}-T_0)+$$

$$+\frac{1}{\Lambda(T_0)}\frac{\partial \Lambda}{\partial P}\Delta P\left(1-\frac{T_{\rm B}-T_0}{T_{\rm fus}-T_0}\right)\Bigg], \quad (19)$$

and the temperature dependence of the LD length has the form

$$L_1(T_{\rm LD}) = L_1(T_0)[1+\alpha_{\rm t}(T_{\rm LD}-T_0)], \quad (20)$$

where $\alpha_{\rm t}$ is the linear expansion coefficient of the LD.

4. Experimental and spectral characteristics of the radiator

Let us list the conditions taken into account when calculating the spectral characteristics of the laser emitter.

(i) Heating of the LD active region by the pump current flowing through it was neglected.

(ii) The FBG and the optical fibre were assumed to have normal dispersion. The values of the phase and group refractive indices for the FBG and fibre at a wavelength of $\lambda = 852$ nm were taken from Fig. 1.4 [6]. This made it possible to determine the quantities $\partial n_2/\partial\lambda$ and $\partial n_{\rm B}/\partial\lambda$, which we consider equal to each other. For the LD the derivative $\partial n_1/\partial\lambda = -7\times10^3$ cm^{-1} is borrowed from [7]. The group refractive index $n_{i\rm gr} = n_{i0} - \lambda_{\rm B}\partial n_i/\partial\lambda$, where $i = 1, 2, B$.

(iii) For the active region of the LD the quantity $n_{10}^{-1}[\partial n_1/\partial T + \Gamma_{\rm a}(\partial n_1/\partial n_{\rm a})(\partial n_{\rm a}/\partial T)]$ was taken to be 0.77×10^{-4} K^{-1}. The quantity $\partial n_1/\partial n_{\rm a}$ takes into account the change in the refractive index due to pump current injection and includes anomalous dispersion, and the contribution of the plasma of free carriers [4].

(iv) The values of μ, E, ρ_{11}, ρ_{12}, $\alpha_{\rm Bt}$ and $n_{\rm B0}^{-1}(\partial n_{\rm B}/\partial T)$ were taken from [8].

In the calculations we used the following parameters: $L_1 = 0.06$ cm, $L_2 = 0.76$ cm, $L_3 = 30$ μm, $L_{\rm B} = 0.4$ cm, $n_{10} = 3.3$, $n_{20} = n_{\rm B0} = 1.452$, $n_3 = 1$, $R_1 = 0.3$, $R_2 = 0.04$, $R_3 = 0.005$, $R_{\rm B} = 0.04$, $\alpha_{01} = 15$ cm^{-1}, $\alpha_{\rm B} = 0.005$ cm^{-1}, $\partial n_2/\partial\lambda = \partial n_{\rm B}/\partial\lambda = -160$ cm^{-1}, $\mu = 0.164$, $E = 7.6\times10^7$ Pa, $\rho_{11} = 0.121$, $\rho_{12} = 0.27$, $\alpha_{\rm Bt} = 5.4\times10^{-7}$ K^{-1}, $\alpha_{\rm t} = 5.74\times10^{-6}$ K^{-1}, $n_{\rm B0}^{-1}(\partial n_{\rm B}/\partial T_{\rm B}) = 6.8\times10^{-6}$ K^{-1}, $\Delta P = 7.95\times10^7$ Pa, $T_0 = 293$ K, $T_{\rm fus} = 387$ K. The missing parameters are taken from [2].

Figure 2a shows the experimental dependence of the radiation wavelength on the LD temperature at a fixed pump current $I = 43$ mA and the FBG temperature $T_{\rm B} = 20\,^\circ$C. One can see that the radiation wavelength changes cyclically over the modes of the LD and the external cavity. Figure 2c illustrates the calculated dependences of changes in the emission spectrum on the LD temperature, while Fig. 2b demonstrates the spectrum of the FBG reflectance modulus that defines the cyclic change in the radiation wavelength and depends on the coupling coefficient of counterpropagating waves K_0. Formula (4) was used to calculate $|r^2|$. One can see that the dependences in Figs 2a and c satisfactorily coincide. Figures 2d, e, and f demonstrate the behaviour of the emission spectrum at points *1*, *2* and *3* (Fig. 2c). The spectral characteristics of the LD with a FBG are presented in a logarithmic scale for the radiation power of 10 mW. Point *1* corresponds to the simultaneous generation of two LD modes, point *2* – two modes of the external cavity, and point *3* – single-frequency generation. The calculation shows that, as in the case shown in Fig. 4 from paper [2], it suffices to deviate from the temperature at points *1* and *2* by 0.1 °C in order to ensure stable single-frequency generation.

The laser emitter spectra shown in Figs 2c–f are calculated for the coupling coefficient of counterpropagating FBG waves $K_0 = 9$ cm^{-1}. Of interest is the analysis of the behaviour of the emission spectrum at different values of K_0. Figures 3b and 4b show temperature dependences of the LD wavelength for the coupling coefficients $K_0 = 15$ and 5 cm^{-1}, respectively, at a constant FBG temperature 20 °C. Figures 3a and 4a present reflectance moduli and FBG

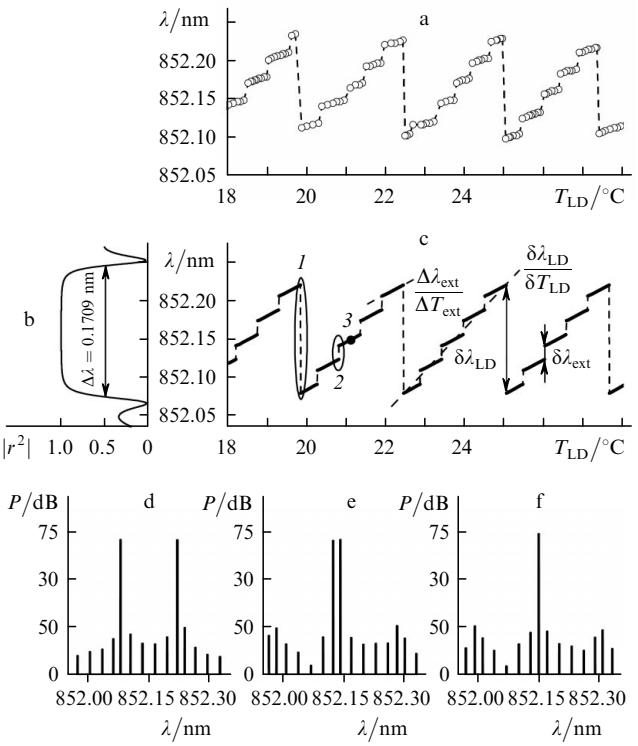

Figure 2. Experimental (a) and calculated (c) dependences of the radiation wavelength of the LD on its temperature at a constant FBG temperature and LD pump current, wavelength dependence of the FBG reflectance modulus (b), and emission spectra at points *1*, *2* and 3 (d, e, f). The coupling coefficient is $K_0 = 9$ cm^{-1}.

reflection wavelength ranges (at the $0.5|r^2|$ level). The spectra at points *1*, *2* and *3* indicated in Figs 3b and 4b, respectively, are shown in Figs 3c, d, e and 4c, d, e.

Comparison of spectral characteristics, presented in Figs 2c, 3b and 4b, shows that they are strongly dependent on the coupling coefficient K_0. A similar conclusion can be drawn for the dependences presented in Figs 2d–f, 3c–e

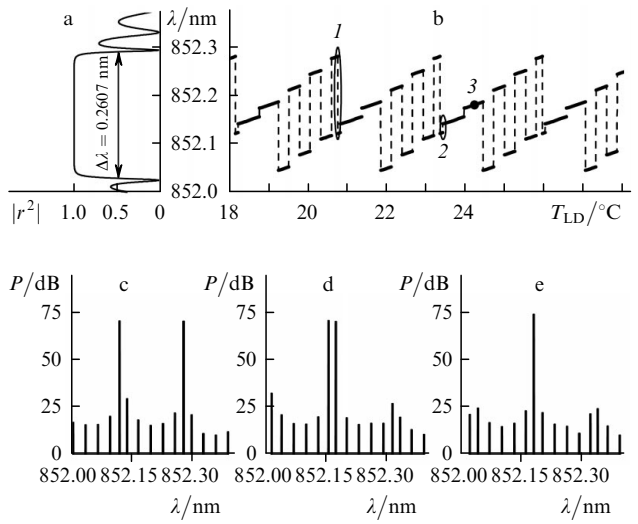

Figure 3. Wavelength dependence of the FBG reflectance modulus (a), calculated dependence of the radiation wavelength of the LD on its temperature at a constant FBG temperature and LD pump current (b) and emission spectra at points *1*, *2* and *3* (c, d, e). The coupling coefficient is $K_0 = 15$ cm^{-1}.

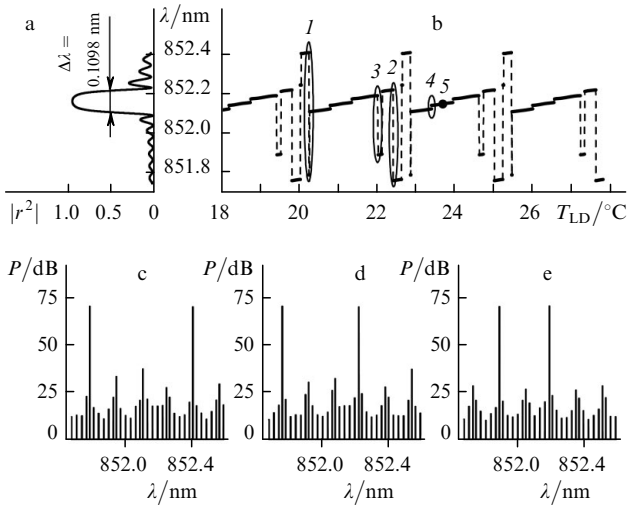

Figure 4. Same as in Fig. 3 but at the coupling coefficient $K_0 = 5$ cm^{-1}.

and 4c–e. It follows from Fig. 4c that the maximum distance between the two generation modes corresponds to four intermode LD intervals. Points *2* and *3* in Fig. 4b correspond to the three and two intermode LD intervals in Figs 4d, e. The asymmetry of the spectrum in Fig. 4b is determined by the asymmetry of submodes $|r^2|$ (for example, in Fig. 4a there are more submodes in the short-wavelength wing $|r^2|$ than in the long-wavelength wing). The emission spectra at points *4* and *5* in Fig. 4b correspond to the emission spectra at points *2* and *3* in Figs 2c and 3b, shown in Figs 2e, f and Figs 3d, e.

Figure 5 presents the experimental and calculated dependences of the wavelength on the FBG temperature at a constant pump current, temperature of the LD and the coupling coefficient $K_0 = 9$ cm^{-1}.

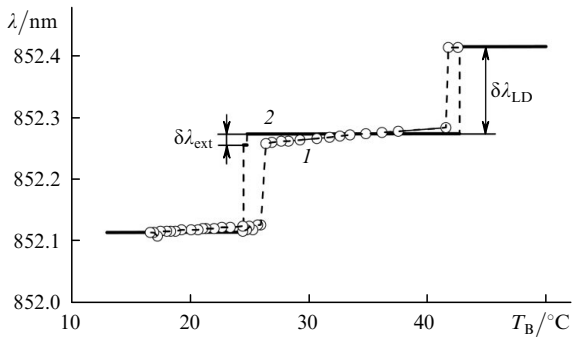

Figure 5. Experimental (*1*) and calculated (*2*) wavelength dependences of the FBG temperature at a constant temperature and pump current of the LD. The coupling coefficient is $K_0 = 9$ cm^{-1}.

5. Discussion of the results

(i) We have found experimentally that the shift of the wavelength $\Delta\lambda_{Bp}(T_0)$ to the blue after soldering the FBG to the TEC is 0.18 nm. Therefore, at $T_B = T_0$ we can determine from (13) the pressure increment $\Delta P = 7.95 \times 10^7$ Pa. The ratio of the wavelength shift to the pressure increment is $\Delta\lambda_{Bp}(T_0)/\Delta P = -2.26 \times 10^{-3}$ nm MPa^{-1}, which correlates with $\Delta\lambda_{Bp}/\Delta P = -3 \times 10^{-3}$ nm MPa^{-1} given in [5].

(ii) Analysis of the calculated and experimental curves presented in Figs 2a and c shows that their temperature period of repetition of the characteristics δT_{LD} coincides and is $\sim 2.6\,^{\circ}C$. Intermode intervals are found from the experimental curve in Fig. 2a: for the LD $\delta\lambda_{LD} \simeq 0.126$ nm and for the external cavity $\delta\lambda_{ext} \simeq 0.021$ nm. Their calculated values are 0.141 and 0.0182 nm, respectively. The rate of change of the wavelength with the LD temperature obtained from the experimental curves is $\delta\lambda_{LD}/\delta T_{LD} \simeq 0.0485$ nm K^{-1}, and for the external cavity $\Delta\lambda_{ext}/\Delta T_{ext} \simeq 0.015$ nm K^{-1}, whereas the calculated values are $\delta\lambda_{LD}/\delta T_{LD} = 0.054$ nm K^{-1} and $\Delta\lambda_{ext}/\Delta T_{ext} = 0.0265$ nm K^{-1} (Fig. 2c). Thus, the dependences in Figs 2a and c satisfactorily coincide.

(iii) Comparison of the curves in Fig. 5 shows that satisfactory agreement between calculations and the experiment is observed in the temperature range $15-45\,^{\circ}C$. However, it should be noted that switching in external cavity modes was not observed in the experiment, although the calculations demonstrate switching in the LD modes and switching in the modes of the external cavity.

(iv) To construct an AFC system, the spread in the wavelengths should be minimal (Figs 2c, 3b and 4b). This is necessary for the system to return to the restore point after possible failure. The spectral characteristics in Figs 2a, c, whose spread in the radiation wavelengths is minimal and coincides with the intermode interval of the LD, meet this condition. The spread in the excited wavelengths in Figs 3b and 4b is much greater than in Fig. 2c; therefore, to design an AFC system it is necessary to select the optimal FBG reflection band, which is presented in Fig. 2b.

(v) It is reasonable to construct an AFC system using the temperature control of the FBG rather than of the LD. Comparison of the experimental dependences in Fig. 2a and Fig. 5 shows that the range of the temperature change for the FBG is much greater than for LD. In addition, in regulating the AFC by varying the FBG temperature, the LD temperature remains constant and can be chosen minimally possible so that to ensure a significant increase in the service life of the laser emitter.

Thus, the developed model of the laser emitter, which takes into account pressure, temperature and dispersion, has made it possible to get satisfactory agreement of the results of experimental and theoretical studies. In constructing the AFC it is advisable to adjust the radiation wavelength by varying the FBG temperature.

References

1. Zhuravleva O.V., Ivanov A.V., Leonovich A.I., et al. *Kvantovaya Elektron.*, **36**, 741 (2006) [*Quantum Electron.*, **36**, 741 (2006)].
2. Zhuravleva O.V., Ivanov A.V., Kurnosov V.D., et al. *Kvantovaya Elektron.*, **38**, 319 (2008) [*Quantum Electron.*, **38**, 319 (2008)].
3. Tsang W.T. (Ed.) *Semiconductor Injection Lasers* (New York: Academic Press, 1985; Moscow: Radio i Svyaz', 1990).
4. Suemutsu Y., Adams A.R. *Handbook of Semiconductor Lasers and Photonic Integrated Circuits* (London: Chapman and Hall, 1994).
5. Rao Y.J. *Meas. Sci. Technol.*, **8**, 355 (1997).
6. Agrawal G. *Nonlinear Fiber Optics* (CA, San Diego: Academic Press, 2001; Moscow: Mir, 1996).
7. Heerlein J., Gruber S., Grabherr M., Jager R., Unger P. *IEEE J. Sel. Top. Quantum Electron.*, **5**, 701 (1999).
8. Okosi T., Okamoto K., et al. *Fibreoptic Sensors* (Leningrad: Energoatomizdat, 1990).